Journal of Power Sources 186 (2009) 299–304

Contents lists available at ScienceDirect

Journal of Power Sources

journal homepage: www.elsevier.com/locate/jpowsour

CO tolerant PtRu–MoO_x nanoparticles supported on carbon nanofibers for direct methanol fuel cells☆

N. Tsiouvaras[a], M.V. Martínez-Huerta[a,b,*], R. Moliner[c], M.J. Lázaro[c], J.L. Rodríguez[b], E. Pastor[b], M.A. Peña[a], J.L.G. Fierro[a]

[a] Instituto de Catálisis y Petroleoquímica, CSIC, Marie Curie 2, 28049 Madrid, Spain
[b] Facultad de Químicas, Universidad de La Laguna, Astrofísico Francisco Sánchez s/n, 38071, La Laguna, Tenerife, Spain
[c] Instituto de Carboquímica, CSIC, Miguel Luesma Castán 4, 50018 Zaragoza, Spain

ARTICLE INFO

Article history:
Received 24 July 2008
Received in revised form
16 September 2008
Accepted 5 October 2008
Available online 17 October 2008

Keywords:
Ternary catalyst
PtRuMo
Carbon nanofiber
CO tolerance
Methanol
Fuel cell

ABSTRACT

Novel nanostructured catalysts based on PtRu–MoO_x nanoparticles supported on carbon nanofibers have been investigated for CO and methanol electrooxidation. Carbon nanofibers are prepared by thermocatalytic decomposition of methane (NF), and functionalized with HNO_3 (NF.F). Electrocatalysts are obtained using a two-step procedure: (1) Pt and Ru are incorporated on the carbon substrates (Vulcan XC 72R, NF and NF.F), and (2) Mo is loaded on the PtRu/C samples. Differential electrochemical mass spectrometry (DEMS) analyses establish that the incorporation of Mo increases significantly the CO tolerance than respective binary counterparts. The nature of the carbon support affects considerably the stabilization of MoO_x nanoparticles and also the performance in methanol electrooxidation. Accordingly, a significant increase of methanol oxidation is obtained in PtRu–MoO_x nanoparticles supported on non-functionalized carbon nanofiber, in parallel with a large reduction of the Pt amount in comparison with binary counterparts and commercial catalyst.

1. Introduction

Direct methanol fuel cells (DMFCs) have been considered to be a favourable option in terms of fuel usage and feed strategies, especially for portable applications, although their commercialization requires further improving of their efficiency and energy density [1]. PtRu nanoparticles supported on carbon black have shown better performance in the methanol electrooxidation than single Pt electrocatalysts [2,3], but these bimetallic systems are not efficient enough and cost competitive for its implementation.

In order to improve the lifetime of the DMFC without increasing cost or losing performance, exploring ternary catalysts and new nanomaterial supporting strategies are some of the most interesting approaches [4]. In a DMFC CO is formed during methanol dissociative adsorption on pure Pt and covers a considerable fraction of the electrode surface. The roles of Ru and the third component are to help in CO oxidation and/or to reduce CO adsorption on Pt [5,6]. In addition, crucial goal of the third component is to replacement of noble metals PtRu, at least partially, by other cheaper and wider disseminated transition metals. Ternary electrocatalysts must be resistant to changes in morphology and surface properties, and their stability may be a determining factor in the useful lifetime of DMFC systems.

PtRuMo electrocatalysts have attracted major attention in recent years [7–16], and promising results have been attained for PEMFC operation with reformate gas and alcohols. PtRuMo nanoparticles are often supported on carbon black (Vulcan XC-72), and occasionally supported on the electronic conducting polymers as polyaniline. However, to our best knowledge, studies of PtRuMo nanoparticles on other nanostructured carbon support have not been reported before.

In this study, carbon nanofibers (NF) and Vulcan XC 72R were compared as support materials for CO and methanol oxidation catalysts. Carbon nanofibers are promising materials as electrocatalyst supports due to their unique properties: resistance to acid/basic media, possibility to control the porosity and surface chemistry, good electrical and mechanical properties [17]. Carbon nanofibers usually contain a negligible amount of oxygen groups, therefore in order to study the effect of the surface oxidation on the structure and the electroactivity of the catalysts, the carbon nanofiber was functionalized with HNO_3 (NF.F). The purpose of the present work

☆ 1st Iberian Symposium on Hydrogen, Fuel Cells and Advanced Batteries (HYCELTEC 2008), 1–4 of July, Bilbao, Spain.

* Corresponding author at: Instituto de Catálisis y Petroleoquímica, CSIC, Marie Curie 2, 28049 Madrid, Spain. Tel.: +34 915854778; fax: +34 915854760.
E-mail address: mmartinez@icp.csic.es (M.V. Martínez-Huerta).

0378-7753/$ – see front matter © 2008 Elsevier B.V. All rights reserved.
doi:10.1016/j.jpowsour.2008.10.026

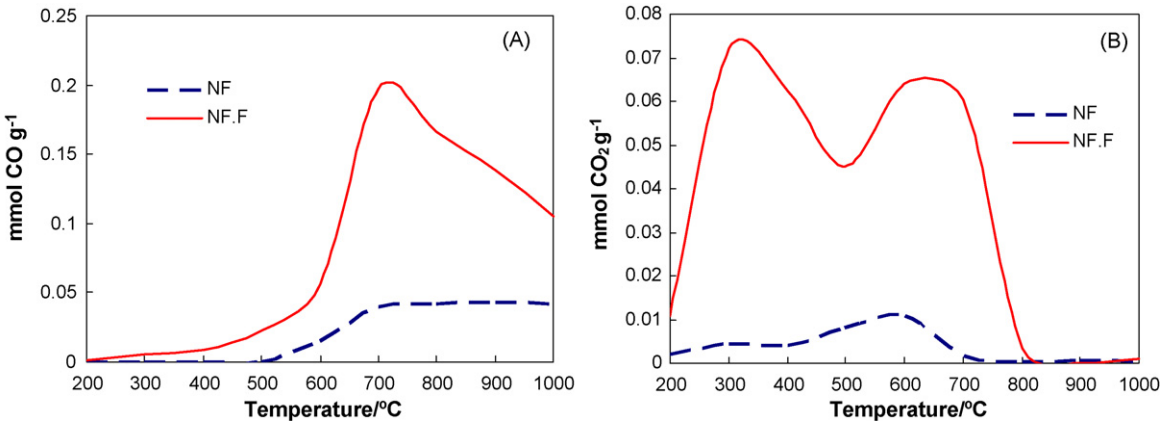

Fig. 1. TPD analysis of carbon nanofibers for CO (A) and CO_2 evolution (B).

is the study of novel nanostructured catalysts based on PtRu–MoO_x nanoparticles supported on carbon substrates (Vulcan XC 72R, NF and NF.F) for CO and methanol electrooxidation. The materials have been prepared using a modification of synthesis method developed by our team via two-step procedure [18]. They have been studied using different physicochemical (XRD, XPS and TEM) and conventional electrochemical techniques such as cyclic voltammetry (CV) and current–time curves applied in combination with differential electrochemical mass spectrometry (DEMS).

2. Experimental

Carbon nanofibers (NF) were prepared by thermocatalytic decomposition of methane at 700 °C for 10 h using a Ni:Cu:Al_2O_3 catalyst. Prior to NF growth, the catalyst was reduced during 3 h at 550 °C in H_2 flow [19]. The functionalized carbon nanofiber (NF.F) was prepared in concentrated HNO_3 (65%) at boiling temperature for 0.5 h. Finally, it was washed with distilled water and dried at 108 °C for 20 h. 30 wt% PtRu (atomic ratio 1:1) electrocatalysts were prepared by sulfito-complex route [20] on Vulcan XC-72R, NF and NF.F. The codes of the resulting electrocatalysts are: PtRu/Vulcan, PtRu/NF and PtRu/NF.F. The ternary catalysts were prepared by adding ammonium molybdate solution (10 wt% nominal Mo content) over different carbon-supported PtRu catalysts in methanol. The suspension was allowed to settle, filtered and dried in an air oven at 110 °C for 12 h. Three catalysts were developed: PtRuMo/Vulcan, PtRuMo/NF and PtRuMo/NF.F. Commercially available electrocatalyst containing 30 wt% PtRu (1:1)/Carbon (Johnson–Matthey) (denoted PtRu/C (JM)) was used for comparison.

Nitrogen adsorption–desorption isotherms of carbon nanofibers were obtained at 77 K using a Micromeritics ASAP 2020. The determination of the amount of surface oxygen groups created during the oxidation treatments was carried out by temperature programmed desorption (TPD) experiments. The amounts of CO and CO_2 desorbed from the carbon samples were analysed by gas chromatography.

Structural characterization of the catalyst was carried out by total-reflection X-ray fluorescence (TXRF, Seifert EXTRA-II spectrometer), X-ray diffraction (XRD, Seifert 3000P X-ray diffractometer), transmission electron microscopy (TEM, JEM-2100F microscope) and photoelectron spectroscopy (XPS, VG Escalab 200R spectrometer).

The electrochemical measurements were carried out at room temperature in a three-electrode cell connected to an electrochemical analyzer (Autolab PGstat 302N). The working electrodes were glassy carbon electrodes for current–time curves (6.0 mm diameter) and for DEMS (7.0 mm diameter) and were prepared according to a modified method developed by Schmidt et al. [21]. The counter electrode was glassy carbon. A reversible hydrogen electrode (RHE) in the supporting electrolyte was employed as the reference electrode for DEMS. For methanol current–time curves, Hg/Hg_2SO_4 was used as the reference electrode, although data in the paper are referenced to the reversible hydrogen electrode (RHE). Differential electrochemical mass spectrometry (DEMS) experiments were carried out in a 2 cm^3 plexiglass flow cell directly attached to the vacuum chamber of the mass spectrometer (Balzers QMG112) provided with a Faraday cup detector. The experimental details are described elsewhere [18]. In all experiments, the working electrode was activated in the supporting electrolyte solution by potential cycling between 0 and 0.80 V and one cycle between 0 and 1.15 V. The anodic stripping of CO adsorbed was studied after bubbling the gas for 15 min while polarizing the electrode at 0.07 V. Oxidation of the adlayer was followed by the mass signal for production of CO_2 ($m/z = 44$). Current–time curves of the electrocatalysts towards methanol oxidation were carried out at 0.45, 0.50, 0.60 V and again 0.45 V in 2 M CH_3OH in 0.5 M H_2SO_4. Current scale was normalized for the electrochemical active surface (EAS) estimated from CO_{ads} stripping voltammetry and realized before each current–time curve at 0.45 V.

3. Results and discussion

Original carbon nanofiber (NF) had a specific surface area of 96 $m^2\,g^{-1}$ and a pore volume of 0.23 $cm^3\,g^{-1}$. The average pore diameter was 7 nm, and micropore volume was negligible. Results from N_2-physisorption showed that the treatment with HNO_3 (NF.F) did not affect significantly the textural properties of NF although its structure was slightly modified. Oxidised NF.F had a specific surface area of 102 $m^2\,g^{-1}$ and a pore volume of 0.21 $cm^3\,g^{-1}$.

Surface chemistry of carbon nanofibers was studied by TPD experiments. These experiments give information about the oxygen surface groups created during the oxidation treatments. Acidic groups are decomposed into CO_2 at lower temperatures and basic and neutral groups are decomposed into CO at higher temperatures. TPD experiments of NF and NF.F are shown in Fig. 1 and proved that surface chemistry of NF.F was modified by the treatment with HNO_3. From the CO_2 evolution peaks it is clear that the number of carboxylic and lactones groups increased significantly, whereas the CO evolution peaks suggested the creation of quinone, phenol and anhydrides groups.

Table 1
Physicochemical characterization of the electrocatalysts.

Catalysts	Atomic ratio Pt/Ru/Mo (TXRF)	Particle size (nm) (XRD)
PtRu/Vulcan	1/1	3.1
PtRuMo/Vulcan	1/0.9/0.7	2.6
PtRu/NF	1/0.9	2.5
PtRuMo/NF	1/0.9/1.2	n.d.
PtRu/NF.F	1/0.9	3.4
PtRuMo/NF.F	1/0.8/0.5	3.1

Atomic ratio Pt/Ru/Mo results of samples using TXRF are compiled in Table 1. It is seen that atomic ratio of Pt/Ru is ca. 1/1 in all samples. However, incorporation of Mo in the binary samples decreases total metal loading, since metal nanoparticles are lost along the filtration step. Higher losses due to the filtration step are observed in Mo species. For Mo-loaded samples, there is a strong dependence of Mo lost on the support, which is higher using functionalized carbon nanofiber (PtRuMo/NF.F). The differences observed in the ternary catalysts could be due to the Mo precursor distribution throughout the carbon support, where the solvent–carbon interaction may play an important role. Therefore, a carbon nanofiber (NF) without oxygen surface groups seems to be capable of a better stabilisation of the Mo species.

X-ray diffraction (XRD) patterns of electrocatalysts are shown in Fig. 2 and reveal the presence of reflections that are assigned to graphite and metallic Ni in carbon nanofibers supports. Electrocatalysts show the characteristic diffraction lines of Pt metal. Moreover, peaks of neither RuO_2, Ru and MoO_x phases are found. The average particle size was estimated according to the Debye–Sherrer equation. For that, the (2 2 0) peak of the Pt fcc structure at $2\theta \sim 67^\circ$ was used (because the broad carbon peak does not interfere in this region). The mean crystallites size were found in the nanoscale range 2–4 nm except PtRuMo/NF, which could not be determined due to the low degree of crystallinity (Table 1).

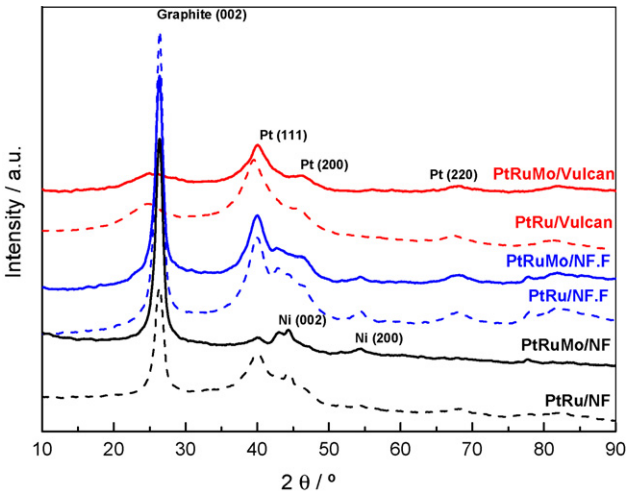

Fig. 2. X-Ray diffraction of electrocatalysts.

Transmission electronic microscopy (TEM) images of ternary catalysts are shown in Fig. 3. Metal particles of PtRuMo/NF catalyst could be determined by TEM and showed a narrow distribution in which the metal particles were predominantly <3 nm. In general, there is a homogeneous distribution with some agglomeration of small particles, and it is characteristic of all ternary samples.

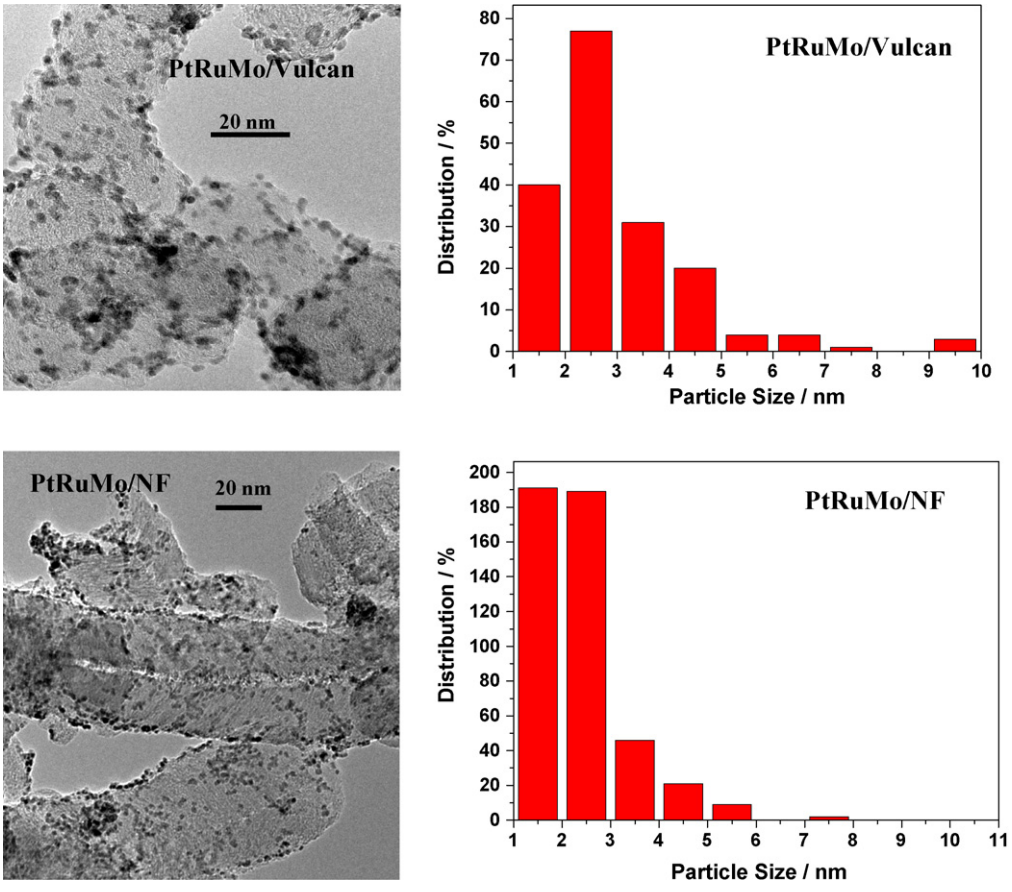

Fig. 3. TEM images of PtRuMo/Vulcan and PtRuMo/NF.

Table 2
XPS results for the electrocatalysts[a].

Catalyst	Pt species	BE of Pt $4f_{7/2}$ (eV)	Ru species	BE of Ru 3p (eV)	Mo species	BE of Mo $3d_{5/2}$ (eV)	Surface metal weight (%) Pt/Ru/Mo
PtRu/Vulcan	Pt (PtO)- PtO_2	71.8 (56) 73.2 (25) 74.7 (19)	RuO_2 RuO_x	463.0 (63) 466.1 (37)			16/9
PtRuMo/Vulcan	Pt (PtO)- PtO_2	71.7 (54) 73.1 (28) 74.8 (18)	RuO_2 RuO_x	463.4 (73) 465.9 (27)	MoO_x MoO_3	232.0 (61) 232.9 (39)	12/7/8
PtRu/NF	Pt (PtO)- PtO_2	71.6 (51) 73.1 (35) 74.8 (14)	RuO_2 RuO_x	463.0 (73) 466.1 (27)			23/11
PtRuMo/NF	Pt (PtO)- PtO_2	71.7 (52) 73.2 (30) 74.8 (18)	RuO_2 RuO_x	463.4 (69) 466.1 (31)	MoO_x MoO_3	232.0 (69) 233.2 (31)	12/9/7
PtRu/NF.F	Pt (PtO)- PtO_2	71.7 (35) 73.1 (45) 74.9 (20)	RuO_2 RuO_x	463.4 (64) 466.1 (36)			21/11
PtRuMo/NF.F	Pt (PtO)- PtO_2	71.6 (44) 72.9 (38) 74.7 (18)	RuO_2 RuO_x	463.4 (76) 465.9 (24)	MoO_x MoO_3	232.1 (66) 233.3 (34)	12/8/8

[a] Numbers in brackets represent the percentage of the corresponding component.

Photoelectron spectroscopy analysis was used in order to get further information on the catalysts surface including the oxidation state of the elements (Table 2). This information must be interpreted taking into account its limitations since the catalysts oxidation state probably change during the electrochemical process. The Pt 4f signal doublets in all samples are derived from three pairs of Pt species, which are attributed to metallic Pt^0 nanoparticles (71.6–71.8 eV), Pt^{2+} species in PtO and $Pt(OH)_2$-like species (72.9–73.2 eV) and Pt^{4+} (74.7–74.9 eV) [22]. Similar concentrations of Pt species were found in all samples, except for catalysts obtained using functionalized carbon nanofiber as support, where the contribution of metallic Pt^0 decreased. The Ru $3p_{3/2}$ signal of samples derives of two species in similar concentrations in all catalysts assigned to Ru^{4+} in anhydrous RuO_2 (463.0–463.4 eV) and hydrous amorphous $RuO_2{\cdot}xH_2O$ species (465.9–466.1 eV) [23]. The Mo 3d spectra for the PtRuMo/Vulcan, PtRuMo/NF, PtRuMo/NF.F indicate the presence of Mo(VI) in MoO_3 species at 232.9–233.3 eV [22]. BEs at lower values ca. 232.0 eV corresponded to a reduction in MoO_x species. Similar concentrations of molybdenum oxide species were observed in ternary catalysts. The binary catalysts show surface metal loading of ca. 25–30 wt%, with a Pt:Ru atomic ratio of 1:1. The incorporation of Mo led to a reduction of the Pt surface loading when the ternary catalysts supported on carbon nanofibers were prepared (Table 2).

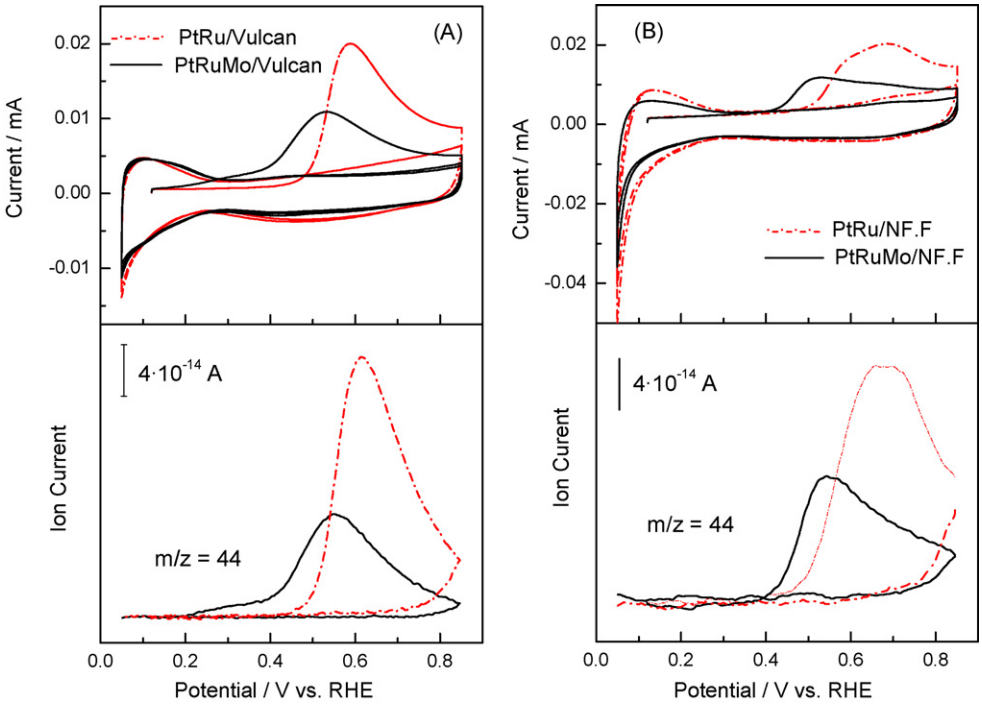

Fig. 4. CV for the oxidation of CO in 0.5 M H_2SO_4 at 25 °C of PtRu/Vulcan//PtRuMo/Vulcan (A) and PtRu/NF.F//PtRuMo/NF.F (B) and the corresponding signal for CO_2 production ($m/z = 44$).

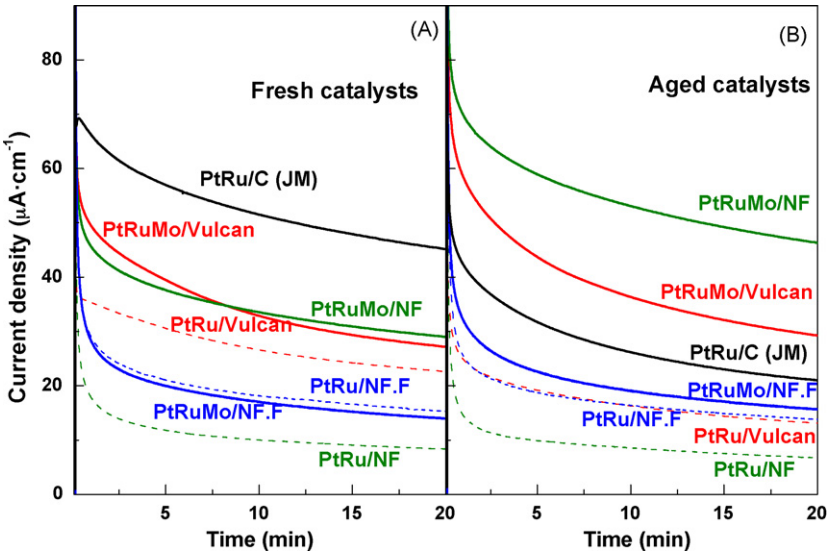

Fig. 5. Current–time curves towards methanol oxidation at 0.45 V of fresh catalysts (A) and aged catalysts (B) in 2 M CH_3OH + 0.5 M H_2SO_4 at 25 °C. Current scale is normalized for the electroactive area estimated from CO_{ads} stripping voltammetry before each current time at 0.45 V.

All Mo-containing catalysts showed a high CO tolerance, with the onset of the CO oxidation to CO_2 being observed at potentials up to 0.10–0.25 V, lower than their binary corresponding catalysts. The DEMS analyses are in accordance with these results. Fig. 4 shows the cyclic voltammetries (CV) for the oxidation of a CO monolayer at PtRu/Vulcan//PtRuMo/Vulcan (A) and PtRu/NF.F//PtRuMo/NF.F (B), and the corresponding signal for CO_2 production (m/z = 44). Similar DEMS analysis to PtRu/NF.F//PtRuMo/NF.F were obtained for coun-

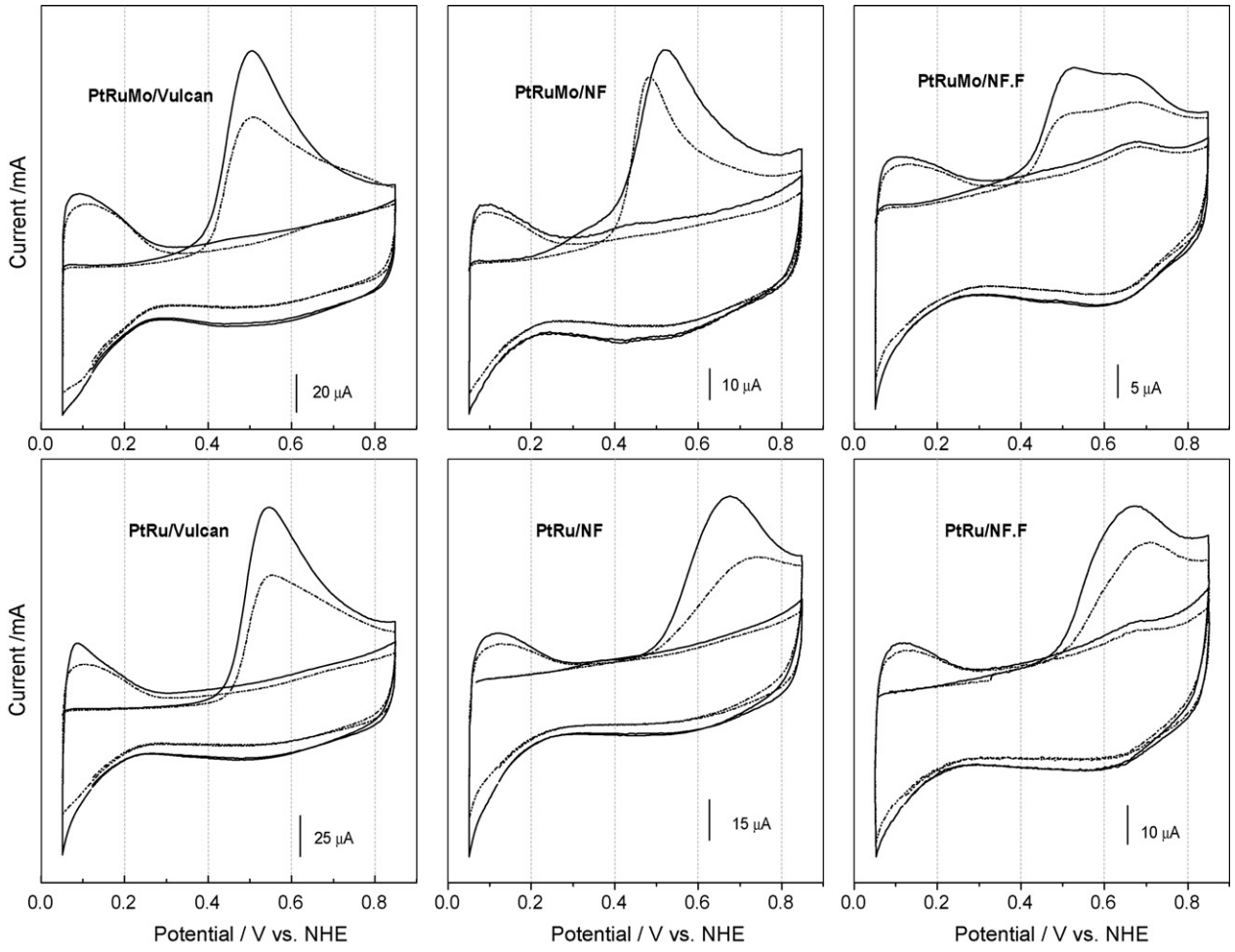

Fig. 6. CV for the oxidation of adsorbed CO of fresh catalysts (—) and aged catalysts (- - - -) before each current time at 0.45 V in 0.5 M H_2SO_4 at 25 °C.

terparts PtRu/NF//PtRuMo/NF (not shown). The lower onset for CO_2 was observed in PtRuMo/Vulcan catalyst and it is established at 0.18 V, which represents a negative shift of about 0.24 V with respect to PtRu/Vulcan catalysts. However, lower currents were obtained in ternary catalysts compared with binary ones, due to the lower surface PtRu loading observed in carbon supported PtRuMo samples.

In order to study the activity and stability of the catalysts and commercial catalyst, PtRu/C (JM), current–time curves towards methanol oxidation were carried out at 0.45, 0.50, 0.60 V and again 0.45 V. Fig. 5 shows current–time dependence at 0.45 V of fresh catalyst (A) and after electrochemical measurements (0.50 and 0.60 V, not shown), denoted as aged catalysts (B). Fresh sample PtRu/C (JM) showed the highest activity followed by fresh ternary PtRuMo/Vulcan and PtRuMo/NF catalysts, which exhibit higher activity than their binary counterparts (Fig. 5A). However, the incorporation of Mo to PtRu/NF.F did not improve the activity for methanol oxidation, even though binary catalyst supported on functionalized carbon nanofiber presented higher activity than PtRu supported on non-functionalized carbon nanofiber. This behavior can be explained on the basis that the functionalized carbon nanofiber hinder the stabilization of the electroactive MoO_x species. It is worth mentioning that after electrochemical measurements (Fig. 5B), the activity of the ternary catalysts rised markedly, especially in PtRu–MoO_x nanoparticles supported on non-funtionalized carbon nanofiber (PtRuMo/NF), if compared with the Mo free catalysts. However, the activity of aged commercial catalyst decreases clearly.

To obtain further information on the active surface area accessible to the reactants of the electrocatalysts, CO_{ads} stripping voltammetry of the fresh and aged catalysts, which were carried out before each current–time curve at 0.45 V, are shown in Fig. 6. The cyclic voltammograms indicated that after electrochemical oxidation of methanol at 0.50 and 0.60 V, electrochemical areas of binary and ternary catalysts decreased markedly. This decrease in CO stripping area suggests that some loss of metals from the surface (presumably Ru and Mo) would occur during the electrochemical measurement due to dissolution. In view of the fact that the activity towards methanol oxidation rises in ternary aged catalysts whereas decreases in binary aged catalysts, it appears that the role of Mo would be crucial for the activation of the electrocatalyst.

For PtRuMo supported on functionalized carbon nanofiber, the CO stripping peak broadened significantly and two peaks were depicted (Fig. 6), which suggests that separate phases are presented in the catalyst. However, when non-functionalized carbon substrates (Vulcan XC 72R and nanofiber) were used, only one CO oxidation peak was observed in PtRuMo/Vulcan and PtRuMo/NF catalysts. The differences between supports, especially the amount of oxygen surface groups, can affect considerably in the molybdenum precursor distribution through the carbon material, where the solvent–carbon interaction may be crucial. Therefore, non-functionalized carbons seem to improve the good proximity and mixing of the molybdenum oxide species on the surface of carbon substrate along with mixed PtRu nanoparticles.

For PtRuMo supported on non-functionalized carbon nanofiber, the CO stripping voltammogram of the aged catalyst showed a small shift in the onset for the electrooxidation to more positive values with respect to the curve corresponding to the fresh catalyst (Fig. 6). This suggests that some MoO_x species, which help to remove preadsorbed CO from PtRu surfaces at lower potentials, were absent in the aged catalyst. However, the CO stripping potential of major peak is shifted to lower potentials, indicative that the catalyst surface became restructured after electrochemical treatment, which has a significant impact on performance in the methanol electrooxidation. The singular properties of carbon nanofibers as high resistance to acid media and good electrical and mechanical properties may play an important role in the activation and stabilization of the PtRuMo nanoparticles. These results point out the importance of the nature of the carbon support as well as its functionalization on the final activity of the electrocatalysts. Nevertheless, further investigations are required in order to understand the nature of the nanostructured PtRu–MoO_x species during electrochemical process and to establish the stability of these materials in a DMFC.

4. Conclusions

Novel CO tolerant PtRu–MoO_x nanoparticles supported on carbon nanofibers, with smaller amount Pt than respective binary counterparts, have been prepared. Carbon nanofibers were prepared by thermocatalytic decomposition of methane, and funcionalized with HNO_3. MoO_x, RuO_x, Pt^0 and PtO_x were the main species revealed by XRD and XPS measurements in the ternary electrocatalysts, whichever the carbon support used including Vulcan XC 72R. Both, the incorporation of MoO_x and the nature of the carbon support affect considerably the performance in methanol electrooxidation, where electrochemical active area and metal nanoparticles stability during operation are key parameters. A significant increase of methanol oxidation is obtained in PtRu–MoO_x nanoparticles supported on non-functionalized carbon nanofiber, due to a major stabilisation of the electroactive MoO_x species over NF.

These results open a new area of investigation where combining the optimization of three-metal system composition and carbon support material, and increase in the efficiency of the electrocatalysts could be achieved.

Acknowledgements

This research was funded by the Ministry of Education and Science, Spain (Projects ENE2007-67533-C02-01, NAN2004-09333-C05-01 and NAN2004-09333-C05-04). The authors wish to thank "FEDER" for its financial support. N.T. acknowledges the I3P program (CSIC) for financial support.

References

[1] A.S. Aricò, R. Srinivasan, V. Antonucci, Fuel Cells 1 (2001) 133–161.
[2] A. Hamnett, Catal. Today 38 (1997) 445–457.
[3] O. Petrii, J. Solid State Electrochem. 12 (2008) 609–642.
[4] A.S. Arico, P. Bruce, B. Scrosati, J.-M. Tarascon, W.V. Schalkwijk, Nat. Mater. 4 (2005) 366–377.
[5] M. Watanabe, S. Motoo, J. Electroanal. Chem. 60 (1975) 267.
[6] T. Frelink, W. Visscher, J.A.R. van Veen, Surf. Sci. 335 (1995) 353.
[7] K. Lasch, L. Jörissen, J. Garche, J. Power Sources 84 (1999) 225–230.
[8] A. Lima, C. Coutanceau, J.M. Leger, C. Lamy, J. Appl. Electrochem. 31 (2001) 379–386.
[9] Z. Jusys, T.J. Schmidt, L. Dubau, K. Lasch, L. Jörissen, J. Garche, R.J. Behm, J. Power Sources 105 (2002) 297–304.
[10] A. Oliveira Neto, E.G. Franco, E. Arico, M. Linardi, E.R. Gonzalez, J. Eur. Ceram. Soc. 23 (2003) 2987–2992.
[11] C.J. Song, M. Khanfar, P.G. Pickup, J. Appl. Electrochem. 36 (2006) 339–345.
[12] Z. Hou, B. Yi, H. Yu, Z. Lin, H. Zhang, J. Power Sources 123 (2003) 116–125.
[13] D.C. Papageorgopoulos, M. Keijzer, F.A. de Bruijn, Electrochim. Acta 48 (2002) 197–204.
[14] M. Götz, H. Wendt, Electrochim. Acta 43 (1998) 3637.
[15] D.A. Stevens, J.M. Rouleau, R.E. Mar, R.T. Atanasoski, A.K. Schmoeckel, M.K. Debe, J.R. Dahn, J. Electrochem. Soc. 154 (2007) B1211–B1219.
[16] T. Kessler, A.M.C. Luna, J. Solid State Electrochem. 7 (2003) 593–598.
[17] P. Serp, M. Corrias, P. Kalck, Appl. Catal. A 253 (2003) 337–358.
[18] M.V. Martínez-Huerta, J.L. Rodríguez, N. Tsiouvaras, M.A. Peña, J.L.G. Fierro, E. Pastor, Chem. Mater. 20 (2008) 4249–4259.
[19] L. Calvillo, M.J. Lazaro, I. Suelves, Y. Echegoyen, E.G. Bordejé, R. Moliner, J. Nanosci. Nanotechnol., in press.
[20] M. Watanabe, M. Uchida, S. Motoo, J. Electroanal. Chem. 229 (1987) 395–406.
[21] T.J. Schmidt, M. Noeske, H.A. Gasteiger, R.J. Behm, P. Britz, H. Bönnemann, J. Electrochem. Soc. 145 (1998) 925–931.
[22] D. Briggs, M.P. Seah, Practical Surface Analysis by Auger and X-ray Photoelectron Spectroscopy, Chichester, 1990.
[23] A.S. Arico, V. Baglio, A. Di Blasi, E. Modica, P.L. Antonucci, V. Antonucci, J. Electroanal. Chem. 557 (2003) 167–176.